International Journal of Mechanical, Industrial and Aerospace Sciences
ISSN: 2517-9950
Vol:6, No:10, 2012

A New Perturbation Technique in Numerical Study on Buckling of Composite Shells under Axial Compression

Zia R. Tahir, P. Mandal

***Abstract*—**A numerical study is presented on buckling and post buckling behaviour of laminated carbon fiber reinforced plastic (CFRP) thin-walled cylindrical shells under axial compression using asymmetric meshing technique (AMT). Asymmetric meshing technique is a perturbation technique to introduce disturbance without changing geometry, boundary conditions or loading conditions. Asymmetric meshing affects predicted buckling load, buckling mode shape and post-buckling behaviour. Linear (eigenvalue) and non-linear (Riks) analyses have been performed to study the effect of asymmetric meshing in the form of a patch on buckling behaviour. The reduction in the buckling load using Asymmetric meshing technique was observed to be about 15%. An isolated dimple formed near the bifurcation point and the size of which increased to reach a stable state in the post-buckling region. The load-displacement curve behaviour applying asymmetric meshing is quite similar to the curve obtained using initial geometric imperfection in the shell model.

***Keywords*—**CFRP Composite Cylindrical Shell, Finite Element Analysis, Perturbation Technique, Asymmetric Meshing Technique, Linear Eigenvalue analysis, Non-linear Riks Analysis

I. Introduction

THE composite thin-walled cylindrical shells are generally used as load carrying components in various structures due to their significant strength-to-weight ratio. These thin walled structures are usually subjected to compressive loads and buckling behaviour is the key design criteria. The thin cylindrical shells have a large number of imperfections due to fabrication process and loading arrangements usually termed as geometrical, material, loading and other imperfections. The geometric imperfections include non-uniform thickness, local indentations, dents, cracks, non-circularity and non-cylindricity in the shell structures. The material imperfections include non-homogeneity, impurities and vacancies; loading imperfections include eccentricity in loading, where as other imperfections include residual stresses and strains induced due to manufacturing processes. All these imperfections affect the load carrying capacity of shell structures but geometrical imperfections in particular.

Zia R. Tahir is with the Mechanical Engineering Department, University of Engineering and Technology, Lahore, Pakistan currently doing Ph.D. from School of Mechanical, Aerospace and Civil Engineering, University of Manchester, UK. (Corresponding Author: phone: +44 7411756328; e-mail: ziartahir@ uet.edu.pk)

P. Mandal is with the School of Mechanical, Aerospace and Civil Engineering, University of Manchester, UK.
(e-mail: p.mandal@manchester.ac.uk)

Asymmetric meshing technique (AMT) is considered to be a perturbation method to introduce disturbance without changing geometry, boundary conditions or loading conditions along with traditional perturbation methods to introduce external disturbance such as initial geometric imperfections, loading conditions or initial material imperfections. In case of asymmetric meshing technique the effect is similar to that caused by the initial geometric imperfection, but it does not cause any asymmetry in loading. Asymmetric meshing affects only the stiffness matrix **K** and does not affect the loading vector **F** in **F** = **Kx** relationship.

Asymmetric meshing had been employed in the numerical shell model without knowing its effect on buckling behaviour of shell structures by many researchers [1-7]. Kim and Kedward [1] used finer mesh in the central circular delaminated region of the rectangular plate compared with rest of plate, while studying the local and global buckling of delaminated composite plates. Cai, Holst and Rotter [2] used convergent mesh to study the buckling behaviour of thin cylindrical shells under localized axial compression. Tafreshi [3] and Han, Cheng, Taheri and Pegg [4] used asymmetric meshing to study the effect of rectangular cut-out (at the mid length of shell) on the buckling behaviour of composite cylindrical shells and aluminum cylinders respectively. Estekanchi and Vafai [5] and Vaziri [6] used asymmetric meshing to model crack in the mid height of composite shell to study its effect on buckling behaviour under axial compression, a fine mesh was used to in cracked region. Prabu, Raviprakash and Venkatraman [7] used asymmetric meshing to model short carbon steel cylindrical shell with dent to study the effect of dent on buckling behaviour, a fine mesh was used in dent region compared with the rest of shell.

Asymmetric meshing technique (AMT) was introduced by Wardle to solve a type of shell buckling benchmark problem [8]. The numerical solution proposed by Sabir and Lock [9] was supposed to be the benchmark solution for circular cylindrical shell section (panel) but Wardle showed it as incorrect by giving a new numerical solution using STAGS (STructural Analysis of General Shells). While solving the incorrect benchmark problem, the main concern was to traverse the bifurcation point and to calculate the associated correct post-bifurcation response by triggering bifurcation using various techniques. Wardle [10] used traditional techniques (geometric or loading imperfection) and asymmetric meshing technique for triggering bifurcation.

The asymmetric meshing technique was considered to be efficient method as complete solution for a given cylindrical shell problem was solved in a single finite element analysis whereas traditional techniques (introducing geometric imperfection) require 5-10 runs after interpreting the prior run's results; that is, the user must adjust amplitude of geometric imperfection so that it is large enough to cause bifurcation but not so large as to change the problem [11]. Wardle [12] calculated the large-deflection buckling behaviour of composite shell structures by the use of finite element method with asymmetric meshing technique for the induction of bifurcation point. asymmetric meshing technique does not impose bifurcation but allows evaluating the bifurcation point and post-buckling accurately and efficiently if it exists in the structural response.

Zhang and Gu [13] used asymmetric meshing technique to study the effect of asymmetric meshing on the predicted primary and secondary buckling behaviour of composite cylindrical shell under axial compression. They concluded that different type of asymmetric meshing have a little influence on the predicted secondary buckling load and have no effect on the linear buckling behaviour of composite shell as geometry, boundary conditions or load has not been changed. Tahir and Mandal [14] used asymmetric meshing technique to study the effect of asymmetric meshing on the predicted buckling load and buckling behaviour of composite laminated cylindrical shells under axial compression. They concluded that asymmetric meshing affects buckling loads, buckling mode shapes and load-deflection curve behaviour in post-buckling region; by applying small asymmetry in meshing there is a variation of 7% in buckling load which increase further by increasing asymmetry in meshing; the different methods of AMT have some influence on predicted buckling load and significant influence on load displacement curve in post-buckling; AMT in axial direction and AMT in circumferential direction have different influence on buckling load and load displacement curve in post-buckling; the effect of AMT is different for shells having same R/t and L/R ratios but different lay-up orientations.

The formation of isolated dimple had been observed during experimental studies by Hambly and Calladine [15]; Mandal and Calladine [16]; Lancaster, Calladine and Palmer [17]. Hambly and Calladine [15] performed experiments on damaged cylindrical shells under axial compression and observed that during buckling process a small size dimple grew near the damaged zone and then turned into a diamond shape. Mandal and Calladine [16] during the experiments on open topped cylindrical shells under self weight buckling observed formation of isolated dimple during buckling and from numerical study using non-linear analysis they observed that during buckling a dimple started to develop near the base of shell as the buckling load reaches the maximum value and then grew in size with decrease in load to reach a stable state.

Bisagni [18] performed experiments on composite laminated cylindrical shells subjected to axial compressive load. Four shells made of carbon fabric with lay-up orientations of $[0^o/+45^o/-45^o/0^o]$ with R/t equal to 265 were tested.

The ratio between experimental and analytical buckling load was in range from 0.63 to 0.72. This experimental data is used for numerical analysis in this paper.

In the present study the effect of asymmetric meshing on the buckling and post buckling behaviour of composite cylindrical shell subjected to axial compressive load are studied with emphasis on the following points:

- Two types of finite element analysis are utilized: linear analysis (Eigenvalue) and non-linear analysis (Riks).
- AMT in the form of a patch is studied for three different cases by varying the size of patch and each patch is then studied for four different degrees of asymmetry.
- The buckling loads from linear and non-linear analysis using asymmetric meshing techniques are compared with the buckling load using symmetric meshing and are presented in form of load factor Λ_N.

II. Numerical Model

The numerical model of composite cylindrical shell considered in this study was a four-ply laminated shell used in the buckling experiments performed by Bisagni [18]. The four specimens of composite cylindrical shell were fabricated from carbon fiber reinforced plastic (CFRP) laminates having both internal diameter and overall length equal to 700 mm, with two tabs at bottom and top surfaces provided for attaching them to loading arrangements. The actual length of the specimens was 520 mm and the nominal thickness of shell wall was 1.32 mm. The radius to thickness ratio (R/t) was equal to 265 and length to radius ratio (L/R) was equal to 1.5. The cylindrical shell has lay-up orientations as $[0^o/45^o/-45^o/0^o]$ and mechanical properties of CFRP are presented in Table 1.

The finite element analysis [19] was used to analyse the buckling and post-buckling behaviour of cylindrical shell under axial compression. The computer program ABAQUS [20] was used for finite element analysis. The shell element S4R was selected, which is a four node reduced-integration shell element having six degrees of freedom at each node, three translational displacements in the nodal directions and three rotational displacements about the nodal axes. The boundary conditions were taken as: all three translational displacements and three rotational displacements were fixed at bottom of shell while only axial translational displacement is free at top of shell. The axial compressive load was transferred to uniform nodal forces along the circumference of the shell.

TABLE I
Mechanical Properties of the CFRP

Elastic Modulus	E_{11}	52000N/mm^2
Elastic Modulus	E_{22}	52000N/mm^2
Shear Modulus	G_{12}	2350 N/mm^2
Poisson's Ratio	ν_{12}	0.302
Density		1320 kg/m^3
Thickness		0.33 mm

The buckling phenomenon had been investigated by eigenvalue analysis. The eigenvalue analysis estimates theoretical buckling load (bifurcation load) of perfect linear elastic structure.

The mesh sensitivity of finite element model had been initially studied for the model using linear (eigenvalue) analysis. The results were verified by comparing with the analytical results given in [21]. The critical buckling load converges well when 52×220 elements (52 elements in the axial direction and 220 in the circumferential direction) were used and the difference with the analytical result is about 4%. The fundamental buckling mode shape of the model with 52×220 elements exhibits a doubly periodic (diamond) shape with 7 axial half waves and 14 circumferential waves. The numerical model of shell with 28×120 elements (28 elements in axial direction and 120 elements in circumferential direction) was analysed as it gave a reasonable agreement between CPU time and precise results. The fundamental buckling mode shape of the model with 28×120 elements exhibits a doubly periodic (diamond) shape with 6 axial half waves and 14 circumferential waves and shown in Fig. 1. The results from eigenvalue analysis using symmetric meshing with 28×120 elements are taken as reference load (numerical buckling load using symmetric meshing technique) for further study and are presented in Table II along with analytical buckling loads.

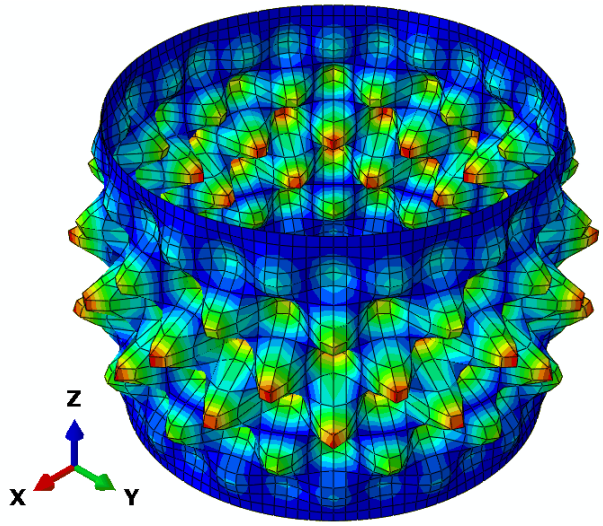

Fig. 1 Fundamental buckling mode shape using symmetric meshing

The buckling phenomenon had also been investigated by non-linear analysis using Riks method [22] or arc length method. In this analysis using ABAQUS, numerical experiments were performed with different load increment (initial arc length increments) from 1% to 0.1% of buckling load with five intervals. During analysis the estimated total arc length is taken as 1 with suitable number of increments to get desire results. Fine load increments were used during numerical simulations as the load becomes equal to the expected critical load estimated by eigenvalue analysis. The approach used in this analysis was to constantly reduce the load increments until the solution starts to converge. The load-displacement curve behaviour changes slightly near buckling in some cases by varying load increments. The Riks analysis is performed for symmetric meshing with 52×220 elements and 28×120 elements and the results are presented in Table II.

The critical load for symmetric meshing was determined by increasing the applied load gradually to find the limit point at which the load end-shortening curve reaches a maximum value of load. The results presented in the Table 2 are the results for buckling load obtained from load end-shorting curve when load reaches its maximum value. The Riks analysis was performed for symmetric meshing with different load increments and the behaviour of load displacement curve was almost same.

TABLE II
COMPARISON AMONG BUCKLING LOADS USING SYMMETRIC MESHING

Solution Type	Buckling Load (kN)
Analytical Solution	240.00
Eigenvalue Analysis (52×220)	248.42
Eigenvalue Analysis (28×120)	274.28
Riks Analysis (52×220)	251.37
Riks Analysis (28×120)	278.81

III. ASYMMETRIC MESHING TECHNIQUE

The numerical model of shell with 28×120 elements (28 elements in axial direction and 120 elements in circumferential direction) with symmetric meshing was analysed using linear (Eigenvalue) analysis and non-linear (Riks) analysis and the results are presented in the Table 2. The shell element in the shell model for symmetric meshing was almost square with width of 18.33 mm in circumferential direction and length of 18.57 mm in axial direction. The shell model using different asymmetric meshing techniques was analysed by using linear analysis and non-linear analysis to study the effect of asymmetric meshing on the linear and non-linear behaviour of shell buckling.

The shell model with asymmetric meshing techniques in the form of a patch is designated as ‘A’ followed by a letter (T, F or S representing patch size) then followed by a number (1, 2, 3 or 4 representing degree of asymmetry in meshing). Asymmetric meshing technique in the form of square patch was employed using three patches of different sizes with four degrees of asymmetry in meshing in each patch explained in Table 3. Three patches were used to produce asymmetry in meshing of the shell model with patch sizes as: ‘T’ (2×2) two elements in circumferential direction and two elements in axial direction with patch size of four elements from symmetric meshing; ‘F’ (4×4) four elements in circumferential direction and four elements in axial direction with patch size of sixteen elements; ‘S’ (6×6) six elements in circumferential direction and six elements in axial direction with patch size of thirty six elements. The numerical model with these three patch sizes are designated as ‘AT’, ‘AF’ and ‘AS’ followed by a number which represents the magnitude of asymmetry in the meshing.

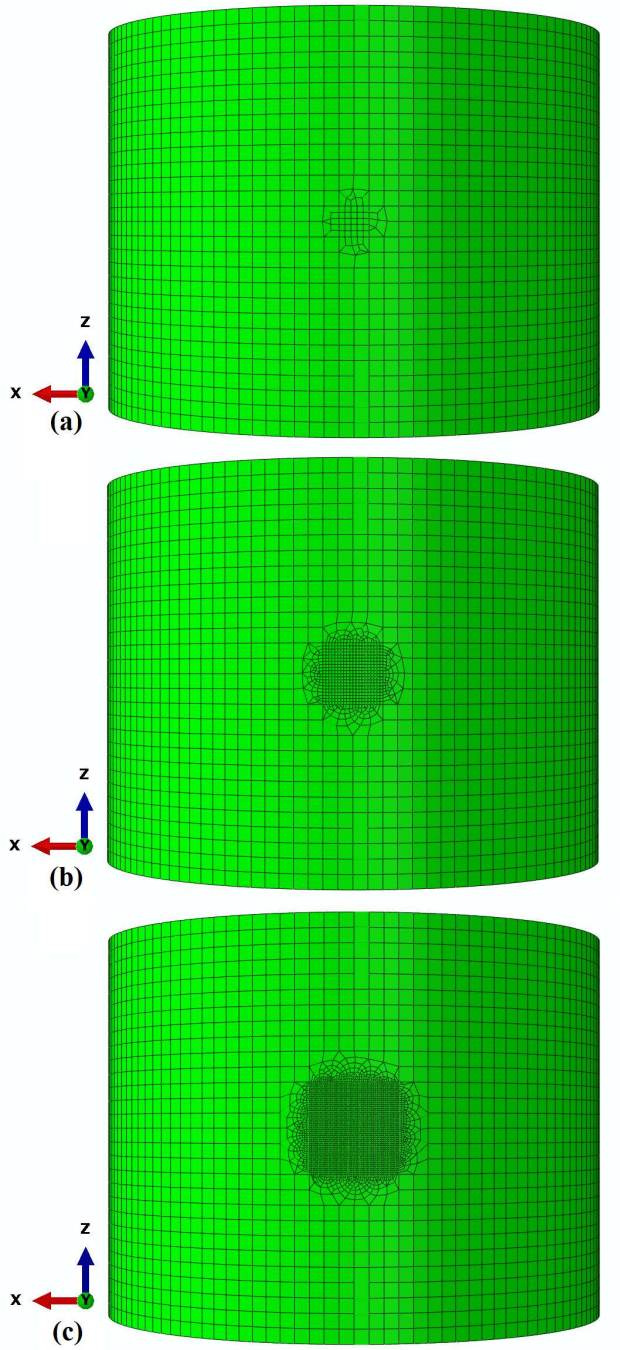

Fig. 2 Asymmetric meshing of numerical model showing patch: (a) AT1; (b) AF2; (c) AS3

For each patch, asymmetry in meshing was produced by reducing the element size in the patch compared with rest of shell model.

The degree of asymmetry in meshing was changed by reducing the element size in patch by four ways as '1' , '2' , '3' and '4'. '1' the element length in the patch was reduced by 2.5 times from the rest of shell model having symmetric meshing (for asymmetric meshing the element length is 2/5 times of element length in symmetric meshing).

Using degree of asymmetry '1'; in 'AT1' 4 elements were converted to 25 elements; in 'AF1' 16 elements were converted to 100 elements; and in 'AS1' 36 elements were converted to 225 elements. Similarly for '2' the element length is reduced by 5.0 times (the element length is 2/10 times of symmetric meshing); '3' the element length was reduced by 7.5 times (the element length is 2/15 times of symmetric meshing); and '4' the element length was reduced by 10.0 times (the element length is 2/20 times of symmetric meshing). The asymmetric meshing in the numerical model in the form of patch for different AMTs is shown in Fig. 2.

TABLE III
EXPLANATION OF THE REPRESENTATION OF NUMERICAL MODELS USING ASYMMETRIC MESHING TECHNIQUE

A T 1

Reduction in element size from symmetric meshing to generate asymmetric meshing
1: ×2/5 **2**: ×2/10 **3**: ×2/15 **4**: ×2/20

Number of elements used for AMT from symmetric meshing
T: 2×2; **F**: 4×4; **S**: 6×6

Asymmetric meshing technique

IV. Linear (Eigenvalue) Analysis

The linear (eigenvalue) analysis had been carried out to study the effect of asymmetric meshing on buckling behaviour. The linear analysis gives the buckling mode shapes and the buckling load for different modes of buckling and in this study the fundamental mode (first mode) was only considered. The results of linear analysis were studied in the form of fundamental buckling mode shape and buckling load. The buckling load from linear or non-linear analysis was normalized with reference load (the buckling predicted by linear analysis using symmetric meshing in the shell model) to give load factor Λ_N. The load factor is the ratio of the numerical buckling load using asymmetric meshing to the numerical buckling load using symmetric meshing.

A. AMT as Patch 'AT'

AMT 'AT' was employed to generate asymmetry in meshing in the patch of size 2×2 (two elements in each direction) and in the patch the element size was reduced to produce four different magnitudes of asymmetry in meshing as 'AT1', 'AT2', 'AT3' and 'AT4'. The buckling mode shape for all AMTs was almost same which was different from mode shape using symmetric meshing (shown in Fig. 1). The axial half-wave length of buckling mode was smaller at mid of the shell near the patch and then increased in both direction towards top and bottom of the shell, the trend was same for half-wave length of buckling mode in circumferential direction as well. The fundamental buckling mode shapes using asymmetric meshing techniques 'AT1' and 'AT4' are shown in Fig. 3. The load factor for 'AT1' is 0.993 and for 'AT4' is 0.989 which shows that using AMT buckling load slightly decreases as compared with symmetric meshing.

The buckling load decreases as the magnitude of asymmetry increases from 'AT1' to 'AT4' and is presented as load factor in Fig. 11a.

B. AMT as Patch 'AF'

AMT 'AF' was employed to generate asymmetry in meshing in the patch of size 4×4 (four elements in each direction) and in the patch the element size was reduced to produce four different magnitudes of asymmetry in meshing as 'AF1', 'AF2', 'AF3' and 'AF4'.

The buckling mode shape for all AMTs was almost same which was different from mode shape using symmetric meshing (shown in Fig. 1). The axial half-wave length of buckling mode was smaller at mid of the shell near the patch and then increased in both direction towards top and bottom of the shell, the trend was same for half-wave length of buckling mode in circumferential direction as well.

The fundamental buckling mode shapes using asymmetric meshing techniques 'AF1' and 'AF4' are shown in Fig. 3. The load factor for 'AF1' is 0.978, for 'AF2' is 0.972, for 'AF3' is 0.972 and for 'AT4' is 0.968 which shows that using AMT buckling load decreases about 3% as compared with symmetric meshing. The buckling load decreases as the magnitude of asymmetry increases from 'AF1' to 'AF4' and is presented as load factor in Fig. 11a.

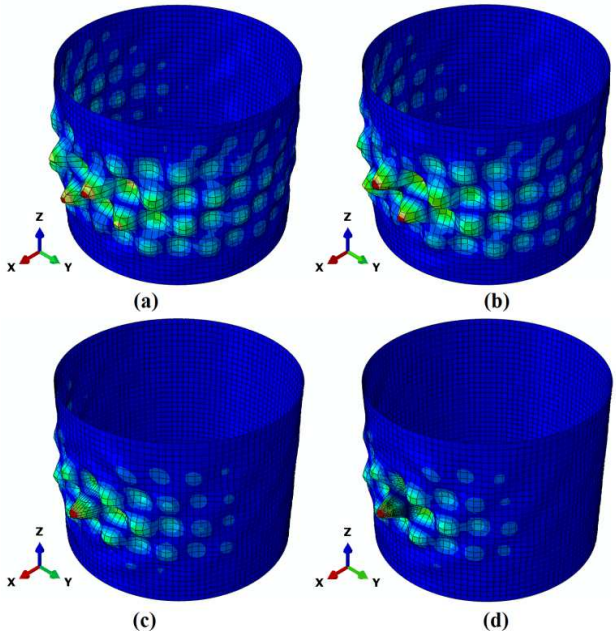

Fig. 3 Fundamental buckling mode shape using AMT:
(a) AT1; (b) AT4; (c) AF1; (d) AF4

C. AMT as Patch 'AS'

AMT 'AS' was employed to generate asymmetry in meshing in the patch of size 6×6 (six elements in each direction) and in the patch the element size was reduced to produce four different magnitudes of asymmetry in meshing as 'AS1', 'AS2', 'AS3' and 'AS4'. The buckling mode shape for all AMTs was almost different and also different from mode shape using symmetric meshing (shown in Fig. 1).

The fundamental buckling mode shapes using asymmetric meshing techniques 'AS1' to 'AF4' are shown in Fig. 4. The load factor for 'AS1' is 0.958, for 'AS2' is 0.952, for 'AS3' is 0.949 and for 'AS4' is 0.948 which shows that using AMT buckling load decreases about 5% as compared with symmetric meshing. The buckling load decreases as the magnitude of asymmetry increases from 'AF1' to 'AF4' and is presented as load factor in Fig. 11a.

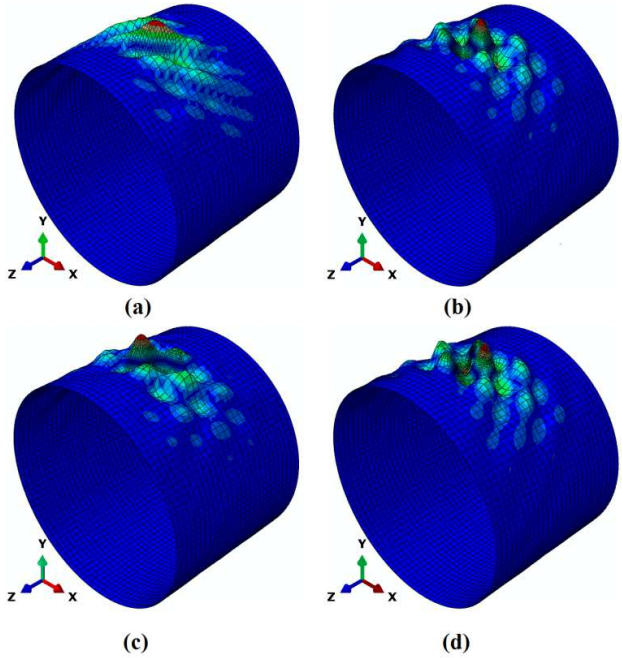

Fig. 4 Fundamental buckling mode shape using AMT:
(a) AS1; (b) AS2; (c) AS3; (d) AS4

V. Non-linear Analysis (RIKS)

The non-linear (Riks) analysis had been carried out to study the effect of asymmetric meshing on buckling and post-buckling behaviour. The non-linear analysis gives the buckling load, buckling mode shape and load-displacement behaviour of the curve in buckling and post-buckling regions. The results of non-linear analysis were studied in the form of buckling mode shape from buckling to post-buckling region, buckling load in terms of load factor and load-displacement curve behaviour. The axial displacement (z), downward displacement from top of shell to bottom, was measured for the node selected at the top edge of the shell above the centre of the dimple. The radial displacement (r), inward displacement, was measured for the node selected at centre of the dimple. The axial displacement and radial displacement are normalized with shell wall thickness (t) to give (z/t) and (r/t) respectively and are plotted against load factor to explain load-displacement behaviour in post buckling region.

A. AMT as Patch 'AT'

The buckling load using asymmetric meshing in from of patch 'AT' is much reduced as compared with buckling load using symmetric meshing.

The load factor for both 'AT1' and 'AT2' is 0.851, for 'AT3' is 0.850 and for 'AT4' is 0.848 and is presented in Fig. 11b. The reduction in buckling load for all AMTs is about 15% and buckling load slightly decreases as the magnitude of asymmetry increases from 'AT1' to 'AT4'. From these results it is observed that reduction in buckling load more depends on patch size and less depends on the magnitude of asymmetry in meshing in the patch.

During buckling an isolated dimple starts to grow above the patch at the ¾ of the length of the shell corresponds to the bifurcation point and then increases to reach a stable state. The dimple formation (from start to reaching stable state) for 'AT1' in the form of radial displacement (mm) is shown in Fig. 4. The shell was modelled using rectangular coordinates system but the results are transformed into cylindrical coordinates system. The corresponding buckling load for each increment shown in the Fig. 5 is taken as percentage of peak load. The peak load is the maximum load obtained from the load displacement curve corresponding to the bifurcation point. Fig. 5a represents the bifurcation point, at this point the maximum radial displacement is at the patch in outward direction and dimple starts at ¾ of the shell height. After the bifurcation point the dimple starts to grow with decrease in buckling load equal to 92% of peak load shown in Fig. 5b, Fig 5c represents the growing of dimple with further reduction in buckling load equal to 57% of the peak load. The buckling load further reduces to a minimum value 36% of the peak load with maximum inward radial displacement shown in Fig. 5d. The size of dimple slightly reduces to reach a stable state with a slight increase in buckling load equal to 37% of peak load, the shape of dimple is very similar to that shown in Fig. 5d. The corresponding buckling loads for these buckling states are shown on load-displacement curves in Fig. 7a and Fig. 7b.

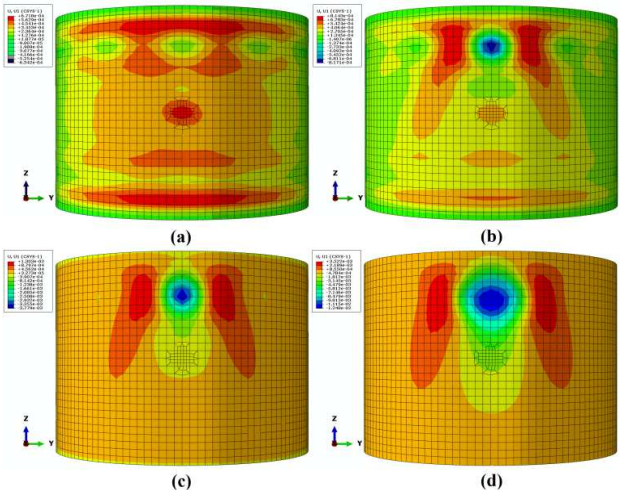

Fig. 5 Buckling mode shape corresponding to peak load: (a) 100%; (b) 92%; (c) 57%; (d) 36%

To study the load versus axial displacement curve behaviour during buckling and post-buckling, eleven nodes were selected on top circumference of the cylinder at the top of dimple and asymmetric patch and these nodes are illustrated in Fig. 6.

The downward axial displacement at these nodes was chosen to plot load-displacement curves which are shown in Fig. 7a. The maximum axial displacement during dimple formation was 1.32 mm (equal to the shell wall thickness) for Node 6 (which is above the centre of the dimple and asymmetric patch) which slightly decreased to 1.1 mm to reach stable state. The axial displacement decreased away from the centre of dimple in both directions with lower values at the edges of dimple. The nodes at the same distance in the opposite direction to the centre of dimple had exactly same load-displacement curve behaviour, and these curves are shown overlapping in Fig. 7a. The load-displacement curve behaviour is quite similar to the curve obtained using initial geometric imperfection in the model and it is observed that applying asymmetric meshing in the model is similar to the introducing geometric imperfection in the model.

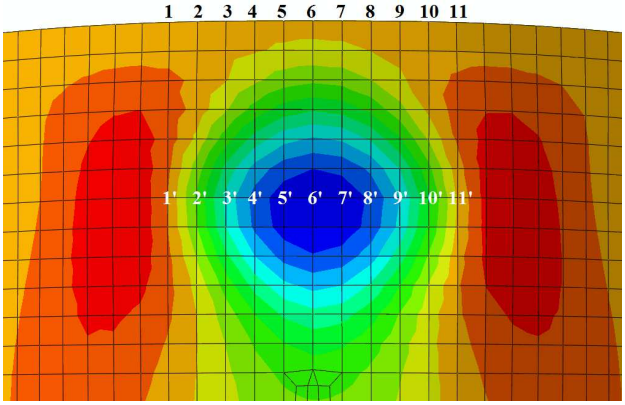

Fig. 6 Close view of dimple showing node numbers on the dimple along circumferential direction and top circumference of model

To study the load versus radial displacement curve behaviour during buckling and post-buckling eleven nodes were selected at the centre of dimple in circumferential direction and are illustrated in Fig. 6. The inward radial displacement at these nodes was chosen to plot load-displacement curves which are shown in Fig. 7b. The maximum radial displacement during dimple formation was 12 mm (equal to nine times the shell wall thickness) for Node 6′ (which was at the centre of the dimple) which slightly decreased to 11 mm to reach stable state. The radial displacement decreased away from the centre of dimple in both directions with lower values at the edges of dimple. The nodes at the same distance in the opposite direction to the centre of dimple have exactly same load-displacement curve behaviour, and these curves are shown overlapping in Fig. 7b.

The phenomenon of dimple formation and growing is slightly different for AMTs from 'AT2', 'AT3' and 'AT4', the dimple start to grow above the patch at the ¾ of the length of the shell, the size of dimple increases at the same position to reach stable state with inward displacement of dimple about 13 mm. The axial displacement (z) and the radial displacement (r) both normalized with shell wall thickness (t) versus load factor for four AMTs are shown in Fig. 8a and Fig. 8b respectively.

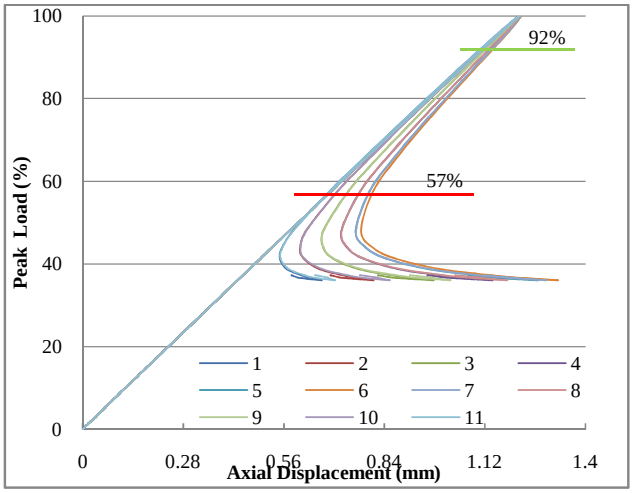

Fig. 7a Peak load versus axial displacement for eleven nodes illustrated in Fig. 6

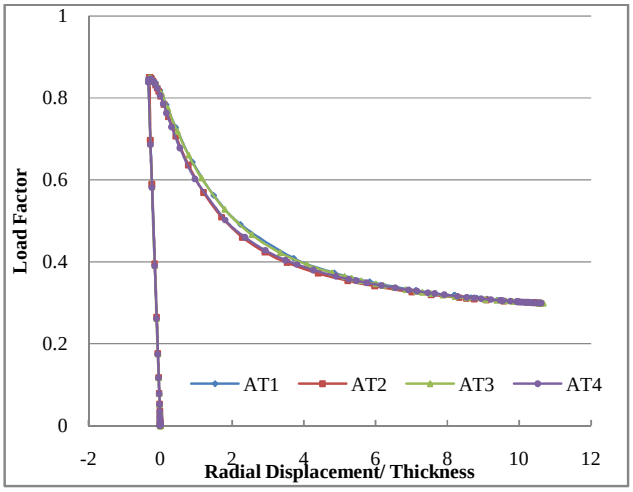

Fig. 8b Load factor versus radial displacement normalized with shell wall thickness for AMT 'AT'

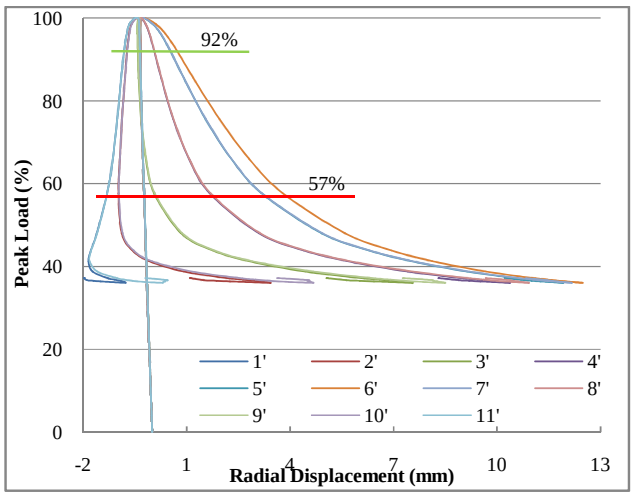

Fig. 7b Peak load versus axial displacement for eleven nodes illustrated in Fig. 6

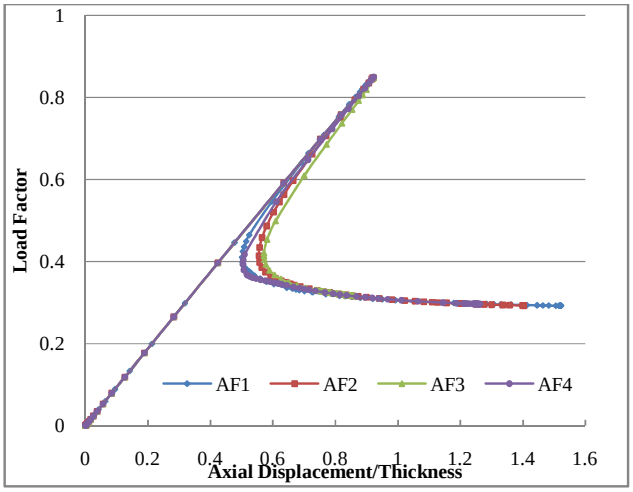

Fig. 9a Load factor versus axial displacement normalized with shell wall thickness for AMT 'AF'

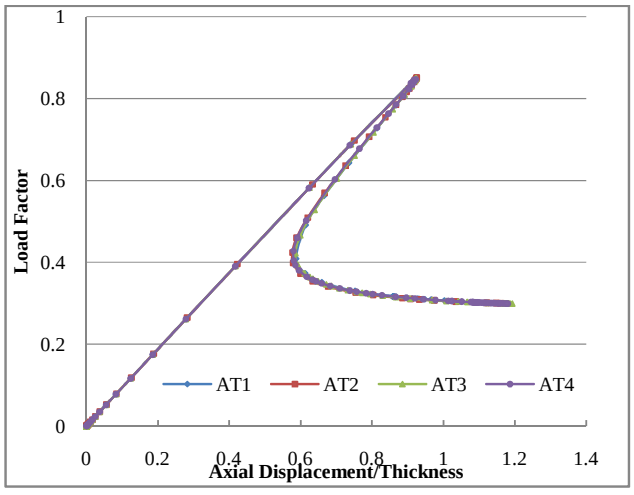

Fig. 8a Load factor versus axial displacement normalized with shell wall thickness for AMT 'AT'

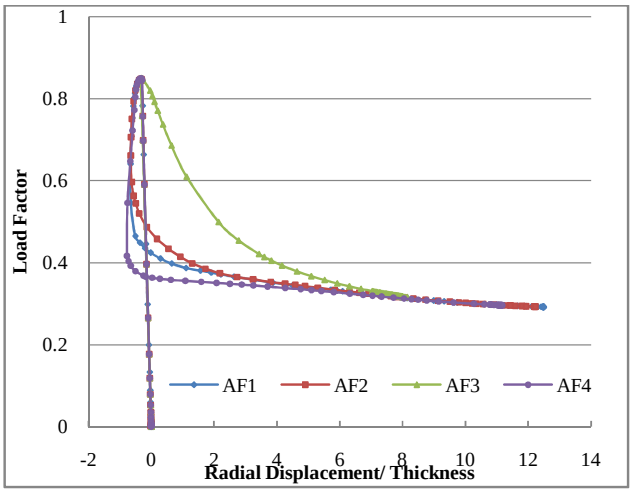

Fig. 9b Load factor versus radial displacement normalized with shell wall thickness for AMT 'AF'

B. AMT as Patch 'AF'

The reduction in buckling load using asymmetric meshing in from of patch 'AF' is much similar to 'AT'. The load factor for both 'AF1' and 'AF2' is 0.850, for 'AF3' is 0.849 and for 'AF4' is 0.847 and is presented in Fig. 11b. The reduction in buckling load for all AMTs is about 15% and buckling load slightly decreases as the magnitude of asymmetry increases from 'AF1' to 'AF4'. From these results it is observed that reduction in buckling load more depends on patch size and less depends on the magnitude of asymmetry in meshing in the patch.

The phenomenon of dimple formation and growing is quite similar for 'AF1', 'AF2' and 'AF4', the dimple starts to grow above the patch at the ¾ of the length of the shell, the size of dimple increases and moves towards the edge of patch to reach stable state with the maximum inward displacement of dimple about 15 mm. For 'AF3' the dimple starts to grow away from the patch at the ¾ of the shell height, the size of dimple increases at the same position with maximum inward displacement of displacement about 9 mm and then decreases to 8 mm to reach stable state. The axial displacement (z) and the radial displacement (r) both normalized with shell wall thickness (t) versus load factor for four AMTs are shown in Fig. 9a and Fig. 9b respectively.

C. AMT as Patch 'AS'

The reduction in buckling load using asymmetric meshing in from of patch 'AS' is slightly different from 'AT' and 'AF'. The load factor for 'AS1' is 0.848, for 'AS2' is 0.845, for 'AS3' is 0.841 and for 'AS4' is 0.831 and is presented in Fig. 11b. The reduction in buckling load for all AMTs is from 15% to 17% and buckling load decreases by 2% as the magnitude of asymmetry increases from 'AF1' to 'AF4'. From these results it is observed that reduction in buckling load more depends on patch size and slightly depends on the magnitude of asymmetry in meshing in the patch.

The phenomenon of dimple formation and growing is quite similar for 'AS1' and 'AS2', the dimple starts to grow away from the patch at the ¾ of the shell height, the size of dimple increases and moves further away from patch to reach stable state with inward displacement of dimple. The maximum inward displacement for 'AS1' is 10 mm which slightly reduces to 9 mm to reach stable state of dimple formation; similarly the maximum displacement for 'AS2' is 9 mm which slightly reduces to 8 mm to reach stable state. For 'AS3' and 'AS4' the dimple formation is quite similar, the dimple start to grow above the patch at the ¾ of the shell height, the size of dimple increases and moves towards the edge of patch to reach stable state with maximum inward displacement of dimple about 21 mm.

The axial displacement (z) and the radial displacement (r) both normalized with shell wall thickness (t) versus load factor for four AMTs are shown in Fig. 10a and Fig. 10b respectively.

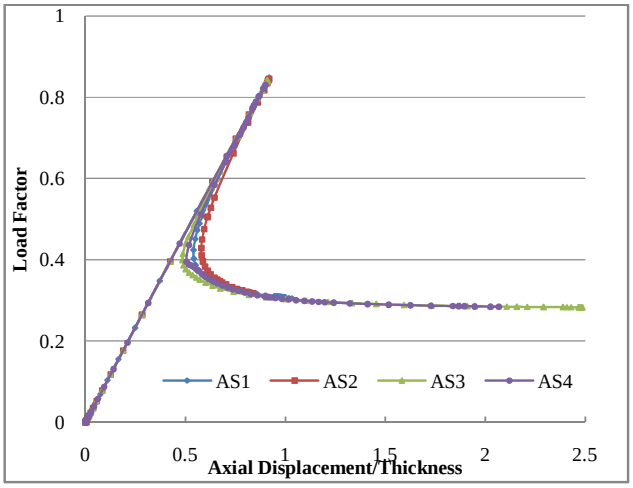

Fig. 10a Load factor versus axial displacement normalized with shell wall thickness for AMT 'AS'

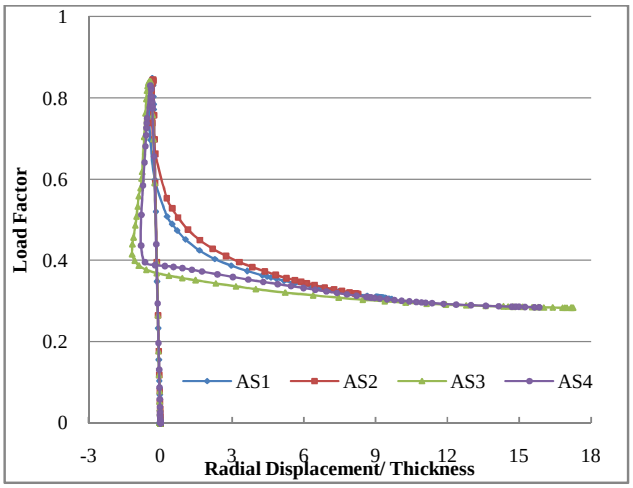

Fig. 10b Load factor versus radial displacement normalized with shell wall thickness for AMT 'AS'

VI. Discussion and Results

The results of asymmetric meshing techniques using linear (eigenvalue) analysis in the form of load factor are shown in Fig. 11a. All AMTs shows same trend in reduction of buckling load as the magnitude of asymmetry increases. The reduction of element size in the patch of particular area leads to reduction in the buckling load. The load factors for AMTs 'AT', 'AF' and 'AS' are 0.99, 0.97 and 0.95 respectively which shows that buckling load decreases as area of patch increases. The trend in the change of buckling mode shapes using AMT is quite similar for all cases; the axial half-wave length and circumferential half-wave length are higher near the patch and decreases as the distance from the patch increases in both directions.

The results of asymmetric meshing techniques using non-linear (Riks) analysis in the form of load factor are shown in Fig. 11b. The trend in reduction of the buckling load is same as discussed above for linear analysis.

The reduction in the buckling load for non-linear analysis is much higher than compared with linear analysis. The effect of AMT on the buckling load for the non-linear analysis is higher than the linear analysis.

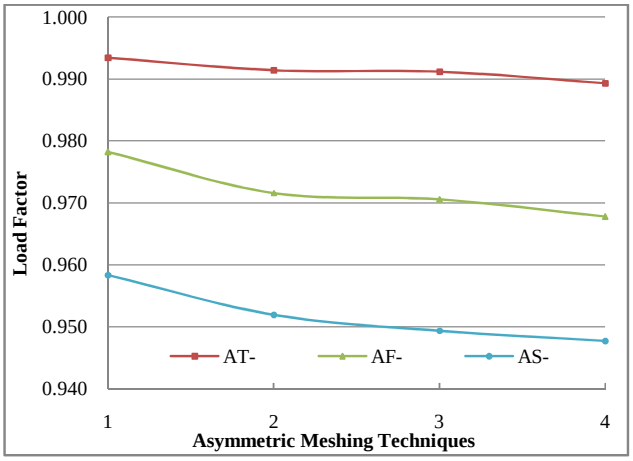

Fig. 11a Load factor for all AMTs using linear analysis

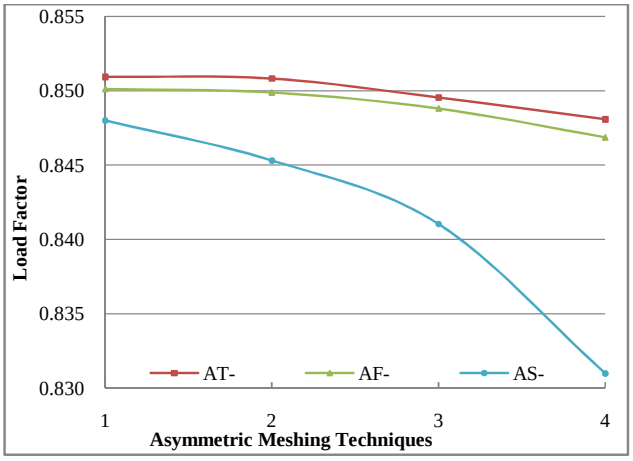

Fig. 11b Load factor for all AMTs using non-linear analysis

The formation of isolated dimple is observed for all cases of asymmetric meshing which is quite similar for all cases, when the buckling load reached a maximum value dimple starts to grow and then grow in size with decrease in buckling load to reach a stable state. In some cases the size of dimple increases to reach a maximum size with a minimum buckling load and then slightly decreases to reach a stable state with slight increase in the buckling load.

In general the size of dimple is almost same for a particular patch size and increases with size of patch and for a particular patch size the magnitude of asymmetry does not affect the size of dimple.

The observation of non-linear analysis of present study when compared with the observation of experimental study on damaged shells under axial compression [15], it is concluded that introducing asymmetric meshing in the numerical model is similar to the creating small dent in the practical shell, in the present study the dimple starts to grow near the patch whereas in [15] the dimple starts to grow near the damaged zone.

The dimple formation and growing observed in the present study is quite similar to the experimental and numerical study performed by Mandal and Calladine [16]. From the present observations and previous observations [15], [16], [17], [23] it is concluded that using asymmetric meshing technique in the numerical model is quite similar to the introducing initial geometric imperfection in the shell model.

VII. Conclusion

Asymmetric meshing affects both bucking loads and buckling mode shapes using linear (eigenvalue) analysis which is different to the previous finding that asymmetric meshing technique has no effect on linear buckling behaviour of composite shells [13]. For non-linear Riks analysis, asymmetric meshing affects buckling loads, buckling mode shapes and load-deflection curve behaviour in post-buckling region. For a particular patch size increasing magnitude of asymmetry in meshing (by reducing the element size in the patch compared with rest of shell) leads to reduction in the buckling load. The buckling load decreases as the size of patch having asymmetric meshing increases. That reduction in buckling load more depends on patch size and slightly depends on the magnitude of asymmetry in meshing in the patch. The dimple formation and growing observed in the present study is quite similar to the previous experimental and numerical study. Asymmetric meshing using in the numerical model is similar to the introducing initial geometric imperfection in the shell model as load-displacement behaviour for both are quite similar.

Acknowledgment

The first author thanks to University of Engineering and Technology, Lahore, Pakistan for financial support for Ph.D. studies under Faculty Development Programme.

References

[1] H. Kim, K.T. Kedward, A method for modeling the local and global buckling of delaminated composite plates, Composite Structures, 44 (1999) 43-53.

[2] M. Cai, M.F.G. Holst, J.M. Rotter, Buckling strength of thin cylindrical shells under localized axial compression, in: 15th ASCE Engineering Mechanics Conference, Columbia University, New York, NY, 2002, pp. 1-8.

[3] A. Tafreshi, Buckling and post-buckling analysis of composite cylindrical shells with cutouts subjected to internal pressure and axial compression loads, International Journal of Pressure Vessels and Piping, 79 (2002) 351-359.

[4] H. Han, J. Cheng, F. Taheri, N. Pegg, Numerical and experimental investigations of the response of aluminum cylinders with a cutout subject to axial compression, Thin-Walled Structures, 44 (2006) 254-270.

[5] H.E. Estekanchi, A. Vafai, On the buckling of cylindrical shells with through cracks under axial load, Thin-Walled Structures, 35 (1999) 255-274.

[6] A. Vaziri, On the buckling of cracked composite cylindrical shells under axial compression, Composite Structures, 80 (2007) 152-158.

[7] B. Prabu, A.V. Raviprakash, A. Venkatraman, Parametric study on buckling behaviour of dented short carbon steel cylindrical shell subjected to uniform axial compression, Thin-Walled Structures, 48 (2010) 639-649.

[8] R.M. Jones, Buckling of Bars, Plates, and Shells, Bull Ridge Corporation, 2006.
[9] A.B. Sabir, A.C. Lock, The applications of finite elements to large deflection geometrically nonlinear behaviour of cylindrical shells, in: C.A. Brebbia, H. Tottenham (Eds.) Variational Methods in Engineering, Southampton University Press, University of Southampton, Southampton, GB, 1972.
[10] B.L. Wardle, Buckling and damage resistance of transversely loaded composite shells, in: Department of Aeronautics and Astronautics, Massachusetts Institute of Technology, Cambridge, 1998.
[11] B.L. Wardle, Solution to the Incorrect Benchmark Shell-Buckling Problem, AIAA Journal, 46 (2008) 381-387.
[12] B.L. Wardle, P.A. Lagace, M.A. Tudela, Buckling response of transversely loaded composite shells, Part 2: Numerical Analysis, AIAA Journal, 42 (2004) 1465-1473.
[13] T. Zhang, W. Gu, The Secondary Buckling and Design Criterion of Composite Laminated Cylindrical Shells, Applied Composite Materials, 19 (2012) 203-217.
[14] Z.R. Tahir, P. Mandal, Effect of Asymmetric Meshing on the Buckling of Composite Laminated Shells, in: International Conference on Advanced Modeling and Simulation, Rawalpindi, Pakistan, 2011, pp. 51-55.
[15] E.T. Hambly, C.R. Calladine, Buckling experiments on damaged cylindrical shells, International Journal of Solids and Structures, 33 (1996) 3539-3548.
[16] P. Mandal, C.R. Calladine, Buckling of thin cylindrical shells under axial compression, International Journal of Solids and Structures, 37 (2000) 4509-4525.
[17] E.R. Lancaster, C.R. Calladine, S.C. Palmer, Paradoxical buckling behaviour of a thin cylindrical shell under axial compression, International Journal of Mechanical Sciences, 42 (2000) 843-865.
[18] C. Bisagni, Experimental Buckling of Thin Composite Cylinders in Compression, AIAA Journal, 37 (1999) 276-278.
[19] K.J. Bathe, Finite Element Procedures in Engineering Analysis, Prentice Hall, New Jersey, 1982.
[20] ABAQUS, Theory and user's manuals, in: Hibbitt, Karlsson, Sorensen. (Eds.), Providence, 2010.
[21] C. Bisagni, Numerical analysis and experimental correlation of composite shell buckling and post-buckling, Composites Part B: Engineering, 31 (2000) 655-667.
[22] E. Riks, An incremental approach to the solution of snapping and buckling problems, International Journal of Solids and Structures, 15 (1979) 529-551.
[23] E. Zhu, P. Mandal, C.R. Calladine, Buckling of thin cylindrical shells: an attempt to resolve a paradox, International Journal of Mechanical Sciences, 44 (2002) 1583-1601.